UPPSALA
UNIVERSITET

UPTEC X 20011
Examensarbete 30 hp
Juni 2020

Spatial and temporal changes in microbial community composition in a full-scale woodchip bioreactor for treating mine water

Felicia Wallnäs

UPPSALA
UNIVERSITET

Teknisk- naturvetenskaplig fakultet
UTH-enheten

Besöksadress:
Ångströmlaboratoriet
Lägerhyddsvägen 1
Hus 4, Plan 0

Postadress:
Box 536
751 21 Uppsala

Telefon:
018 – 471 30 03

Telefax:
018 – 471 30 00

Hemsida:
http://www.teknat.uu.se/student

Abstract

Spatial and temporal changes in microbial community composition in a full-scale woodchip bioreactor for treating mine water

Felicia Wallnäs

Incomplete detonation of nitrogen-based explosives can lead to abundant levels of nitrate in mine groundwater. The possibility of reducing nitrogen levels from the wastewater through denitrification, anammox and DNRA has been investigated using a full-scale bioreactor. The bioreactor is situated subsurface and is filled with pine woodchips. Groundwater is pumped to the bioreactor and subsequently discharged to a drainage ditch. In this thesis the distribution of the microbial community was determined using quantification of functional genes representing a specific functional community. The 16S rRNA gene was used as proxy for the total bacterial community, nirS and nirK for nitrite reduction, nosZI and nosZII genes for nitrous oxide reduction, nrfA for DNRA and the hdh for anammox reaction. Denitrification appeared as the main nitrogen-reducing process in the bioreactor due to more abundant levels of functional genes. The abundance of nitrous oxide reductase was higher than nitrite oxide, indicating good nitrouse oxide reduction. Anammox could not be detected and DNRA was suggested in the end of the bioreactor due to a decrease in nitrate concentration. The distribution of abundances was not affected by the depth or the time which samples were collected. However, abundances collected at different lengths of the bioreactor showed significant differences for 16S rRNA and the functional genes nirS, nosZI and nrfA. This suggests changing environmental conditions along the bioreactor length. Creating an assay for quantification of sulphate reducing bacteria was also investigated. This was not achieved and the size and distribution of the sulphate reducing community remains to investigate. The bioreactor in the present study can reduce nitrogen from mining water but further analysis are needed in order to understand long-term temporal changes.

Handledare: Maria Hellman
Ämnesgranskare: Peter Lindblad
Examinator: Erik Holmqvist
ISSN: 1401-2138, UPTEC X 20011

Populärvetenskaplig sammanfattning

Kväve är ett grundämne som är essentiell för organismer eftersom det utgör en viktig kompent för tillväxt. Förhöjda nivåer av kväve i vatten och jord kan dock leda till bland annat övergödning. Övergödning anses vara ett av de största hoten mot marina miljöer då det leder till ökad tillväxt vilket i sin tur kan leda till syrefattiga miljöer. Inom gruvindustrin är det vanligt att använda kvävebaserade sprängämnen, men vid varje sprängning förblir en del av sprängämnet odetonerat. Efter utvinning av malm från sprängmassorna läggs resten i stora deponier. Vatten från nederbörd löser upp kvävet från odetonerat sprängämne vilket till slut når närliggande vattendrag. Luossavaara-Kiirunavaara Aktiebola (LKAB) använder kvävebaserade sprängämnen. Som ett resultat av detta har förhöjda nivåer av kväve upptäckts i omkringliggande vattendrag. I Sverige har miljömål satts upp i linje med EU:s vattendirektiv där ett av målen är ingen övergödning. För att uppfylla detta mål måste kväveutsläppen till miljön minska.

Detta projekt är en del av projektet NITREM vars syfte är att ta fram en bioreaktorteknik som reducerar kvävenivåer i gruvvatten innan det släpps ut till miljön. Syftet är att bioreaktorn ska göra det möjligt att uppnå de krav som finns på kväveutsläpp till miljön. Tekniken utnyttjar det naturliga mikrobiella samhället, där bakterier har förmågan att reducera kväve genom biokemiska reaktioner i en syrefri miljö. Dessa organismer kan reducera kväve på tre olika sätt; denitrifikation, anaerobisk ammoniumoxidering (anammox) och dissimilatorisk reduktion av nitrat till ammonium (DNRA). Denitrifikation och anammox omvandlar kväve till kvävgas, som 78 % av luften består av, och tar därmed bort kvävet från vattnet. DNRA tar inte bort kvävet från vattnet utan omvandlar endast en kväveförening till en annan.

2018 installerades en bioreaktor hos LKAB i Kiruna. Lakvatten från en stendeponi samlas upp i en vattenreservoar och vattnet pumpas till bioreaktorn, som kan liknas vid ett stort dike fyllt med träflis. Träflisen fungerar som kolkälla för bakterierna. Under sommaren 2019 togs sammanlagt 65 vattenprover från 7 punkter längs vattnets väg genom reaktorn. Proverna togs vid två djup, vid fem tillfällen. Med hjälp av dessa prover ville man undersöka hur effektiv kvävereningen var. Vid provtagning noterades även lukten av vätesulfid, en giftig gas som bildas i en oönskad reaktion där sulfat reduceras. Målet i detta arbete var att undersöka hur fördelningen och storleken av det kvävereducerande mikrobiella samhället såg ut i bioreaktorn. Detta kan förklara vilka av reaktionerna denitrifikation, anammox och DNRA som sker. Ett andra mål var att försöka utveckla en metod för att även undersöka samhället av sulfatreducerande bakterier. Genom att veta vart och hur mycket sulfat som reduceras skulle det öka förståelsen av bioreaktorns prestanda.

I detta projekt bestämdes storleken på det kvävereducerande mikrobiella samhället genom att mäta förekomsten av specifika gener som kodar för enzymer som katalyserar reaktionerna denitrifikation, anammox och DNRA. På så sätt kan fördelningen av de tre olika processerna bestämmas. Statistisk analys utfördes sedan på resultatet för att ta reda på om det fanns skillnader i vilka kvävereducerande processer som fanns i olika delar av bioreaktorn. Resultatet visade att denitrifikation var den huvudsakliga kvävereducerande reaktionen. Det fanns även en tendens för DNRA i slutet av reaktorn men processen anammox kunde inte detekteras. Det mikrobiella samhället skiljde sig mellan olika mätpunkter längs bioreaktorn. Tid och djup tycktes däremot inte påverka storleken av det mikrobiella samhället.

Det andra målet, att ta fram en metod för att undersöka samhället av sulfatreducerande organismer, uppnåddes inte. Storleken och fördelningen av det sulfatreducerande samhället i bioreaktorn återstår att undersöka.

Slutsatsen från detta projekt är att bioreaktortekniken kan reducera kväve från vatten och att den kan vara en hållbar lösning för gruvindustrin. För att veta hur bioreaktorn fungerar på lång sikt behövs fortsatta studier för att undersöka förändringar i det mikrobiella samhället.

Table of contents

Abbreviations

anammox	anaerobic ammonium oxidation
BC	Bray-Curtis
BLAST	basic local alignment search tool
DNA	deoxyribonucleic acid
DNRA	dissimilatory nitrate reduction to ammonium
HRT	hydraulic retention time
LKAB	Luossavaara-Kiirunavaara Aktiebolag
NMDS	non-metric multidimensional scaling
PCR	polymerase chain reaction
SRB	sulphate-reducing bacteria
qPCR	quantitative polymerase chain reaction

1 Introduction

The Swedish Parliament has established environmental goals for sustainable societal developments which include the environmental requirements from the EU water frame directive. One of Sweden's environmental objectives is zero eutrophication (Havs och Vatten Myndigheten, 2020a). Eutrophication is one of the most serious threats to marine environments as it can lead to gradual changes in vegetation and hypoxia (Naturvårdsverket, 2013). In the annual follow-up of the environmental objective Sweden's agency for marine and water management reports a decrease in the excess of nutrients but the levels remain problematic. The recovery time in the environment is long which means it takes time before any improvements can be seen (Havs och Vatten Myndigheten, 2020b). Emissions of nutrients must continue to decrease, and pre-existing nitrogen accumulations must be reduced.

Nitrate-based explosives are common in iron ore mines and lead to the release of nitrogen through leachate mainly from their landfills. At the mining company Luossavaara-Kiirunavaara Aktiebolag (LKAB) nitrate-based explosives are used. Incomplete detonation of ammonium nitrate-based explosives leads to abundant levels of nitrogen in the environment (LKAB, 2019). The quality in water bodies further downstream the discharge of the clarification pond at the mine site is affected with increased levels of nitrate (NO_3^-) and slightly elevated levels of ammonium (NH_4^+) (LKAB, 2019). Additionally, elevated levels of sulphate are also found (LKAB, 2019). This can lead to eutrophication in nearby waters and soils.

The possibility of reducing the nitrogen levels from mining wastewater has been investigated in the project NITREM. The purpose of NITREM is to develop a bioreactor technology that reduces nitrogen levels in leachate from waste rock piles. This technology will make it possible to fulfil the requirements from the Swedish parliament and the EU Water frame directive (NITREM, 2020). The project involves several collaborators, both universities, industries, and stakeholders, in Sweden and in Europe. The bioreactor technology utilises the natural microbial community in the environment to reduce nitrogen. There are three possible nitrogen-reducing reactions which can occur in the bioreactor; denitrification, anaerobic ammonium oxidation (anammox), and dissimilatory nitrate reduction to ammonium (DNRA). Denitrification is the process where NO_3^- is reduced to dinitrogen (N_2). Anammox also creates N_2 but by oxidising NH_4^+ and reducing NO_3^-. In the process DNRA, NO_3^- is reduced to NH_4^+ (Canfield *et al.* 2010).

Previous studies have investigated nitrogen-reduction of mining wastewater in a woodchip bioreactor in the mining company LKAB industrial area in Kiruna, Sweden (Nordström and Herbert, 2018). Mine drainage from a clarification pond at the mine site was pumped to the bioreactor. The study suggested that denitrification was the main nitrogen-reducing pathway but that other unwanted reducing reactions such as DNRA and sulphate reduction were possible. NITREM intends to create a commercial product and is therefore in need of more knowledge about the dynamics in the community composition to better understand the relationship between community structure and performance.

The reactor to be investigated in this thesis is a full-scale bioreactor which was constructed in 2018. It is a woodchip reactor treating nitrate rich drainage collected from a waste rock pile in the mining company LKAB industrial area in Kiruna, Sweden. During water sampling from the bioreactor collected in the summer of 2019, hydrogen sulphide (H_2S) could be detected by its odour at most of the sampling occasions (Maria Hellman, personal communication). However, the sulphate-reducing bacterial community has not been quantified in the present reactor. Quantifying sulphate reducers would increase the understanding of where and to which extent sulphate reduction occurs in the bioreactor.

1.1 Objectives

The first objective of this project was to determine the abundance and distribution of the nitrogen-reducing processes denitrification, anammox, and DNRA in the bioreactor. The abundances were determined by quantification of functional genes which gives an estimation of the size of a specific functional community. The 16S rRNA gene was used as proxy for the total bacterial community, *nirS* and *nirK* for nitrite reduction, *nosZ*I and *nosZ*II for nitrous oxide reduction, *nrfA* for DNRA, and the *hdh* for anammox reaction. The second objective was to develop a qPCR assay for sulphate-reducing bacteria, and to determine their abundance and distribution in the bioreactor.

2 Background

2.1 Nitrate in the mining industry

Explosives used in the mining industry often contain ammonium and nitrate (NH_4NO_3). Under ideal conditions the blasting creates the products water, carbondioxide, and dinitrogen (reaction 1). In reality, nitrogen oxides, such as nitrite (NO_2^-), are also created (Lindeström, 2012). Even though this could contribute to the presence of nitrogen in mine water it is not the primary cause. Leaching from waste rock pile was suggested as the main source of nitrate, as leakage from undetonated explosives easily dissolve in groundwater. In 2012 the estimated share of undetonated explosives at LKAB was 12-13 % (Lindeström, 2012). 20-30 tonnes of explosives are used each day at the Kiruna mine (Nilsson and Widerlund, 2017), resulting in 2-4 tonnes of undetonated explosives every day.

$$3NH_4NO_3 + \frac{1}{2}C_{12}H_{24} \rightarrow 7H_2O + CO_2 + 3N_2 \quad (1)$$

Groundwater which have accumulated in the mine is pumped and discharged in a tailings pond and a clarification pond (Nilsson and Widerlund, 2017). Up to 75 % of the water is however recirculated in production and used when extracting ore from gangue. The surplus of water is discharged to the environment (LKAB, 2019b). In 2019, the release of nitrogen to the recipient was 154 ton, where 136 ton was N in the form of NO_3^- (LKAB, 2019a). In spring, the discharge of mine effluents increases due to snow melt and rainfall. This creates an excessive amount of nitrogen in the environment, more than the nitrogen-reducing organisms can handle, which risks eutrophication (Mattila *et al.* 2007). As previously mentioned, one of Sweden's environmental objectives is zero eutrophication. Another one, which also affects the mining industry, is flourishing lakes and streams (Havs och Vatten Myndigheten, 2020). LKAB reported increase in both size and numbers of the fish population in the recipient, which suggests the effects of eutrophication (LKAB, 2019a).

2.2 The nitrogen cycle

Nitrogen is essential for organisms as it serves as building block in the synthesis of nucleic acids and proteins. It is one of the most abundant elements on earth. However, most of the nitrogen is in the form of molecular nitrogen, a form which is not available

for most organisms. Only some bacteria and archaea have the ability of converting N_2 to readily available nitrogen for living organisms (Galloway *et al.* 2003). Nitrogen-reducing organisms have previously been characterised by which nitrogen-transforming reaction they can perform, but due to more recent analysis of genomic data this needs to be reassessed as a huge versatility in their metabolism has been revealed. The genomic data showed how nitrogen-transforming organisms can carry out different reactions and can therefore not be classified accordingly (Kuypers *et al.* 2018). Nitrogen fixation is the reduction of N_2 to NH_4^+ which requires a large amount of energy (Kuypers *et al.* 2018). Organisms which are incapable of nitrogen fixation obtain nitrogen from their surrounding by available NH_4^+ or through assimilatory NO_3^- reduction where NO_3^- is reduced to NH_4^+. As the organisms die, nitrogen mineralize in the form of NH_4^+ and is returned to the environment. In the presence of oxygen, NH_4^+ is oxidised via intermediates to NO_3^- through nitrification. The greenhouse gas nitrous oxide (N_2O) is a side product in this reaction. In the absence of oxygen, NO_3^- is reduced through either denitrification or DNRA (Canfield *et al.* 2010).

Denitrification is the reduction of NO_3^- to N_2 through a series of reactions, returning nitrogen to the atmosphere (Fig. 1). The pathway occurs in anoxic environments when there is a moderate availability of electron donors in relation to NO_3^- (Canfield *et al.* 2010). In the denitrifying pathway, dissimilatory nitrate reduction is the first step where NO_3^- is reduced to NO_2^-. This is catalysed by either membrane-bound nitrate reductase (NAR) or periplasmic nitrate reductase (NAP) (Kuypers *et al.* 2018). Dissimilatory nitrate reduction does not only occur in organisms which performs denitrification, since many microorganisms use NO_2^- as a source for other nitrogen-cycling processes. In the second step of denitrification, NO_2^- is further reduced to nitric oxide (NO) by nitrite reductase encoded by the functional genes *nir*. NO is reduced to nitrous oxide (N_2O) by nitric oxide reductase, encoded by *nor*. Lastly, N_2O is reduced to N_2 by nitrous oxide reductase encoded by the functional genes *nosZ*. N_2O is a greenhouse gas and *nosZ* is the only known enzyme to catalyse this reaction (Kuypers *et al.* 2018). Some bacteria are not capable of complete reduction and cannot reduce N_2O to N_2 while other bacteria can only perform the last reaction step (Canfield *et al.* 2010).

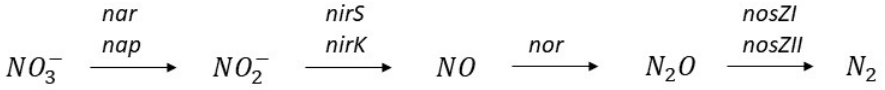

Figure 1: Denitrification and the respective genes catalysing each reaction.

The main reaction in DNRA is dissimilatory nitrite reduction to ammonium. NO_3^- is

reduced through DNRA (Kuypers *et al.* 2018) to NH_4^+ by nitrite reductase encoded by the genes *nrf* (Canfield *et al.* 2010) (Fig. 2). When there is an abundance of electron donors relative to NO_3^-, DNRA appears to be preferred over denitrification (Kuypers *et al.* 2018). The most activating condition for DNRA is a negative redox potential (Stein and Klotz, 2016).

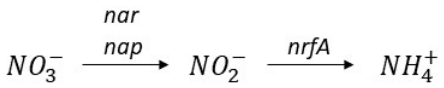

Figure 2: Dissimilatory nitrate reduction to ammonium and the genes catalysing the reaction.

Anammox is a relatively recent discovery and can only be performed by anaerobic ammonium-oxidising bacteria. Anammox is another way of forming N_2 where NH_4^+ is oxidised and NO_2^- reduced in a two-step reaction. The reaction is carried out by the enzyme hydrazine synthase (HZS), encoded by *hzs*, forming the intermediate hydrazine (N_2H_4). In the last reaction step, hydrazine is oxidised to N_2 encoded by the gene hydrazine dehydrogenase, *hdh* (formerly called *hzo*) (Fig. 3), which is responsible for a large release of N_2 to the atmosphere (Kuypers *et al.* 2018).

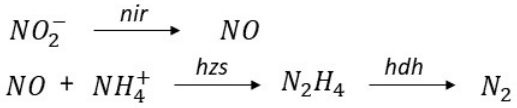

Figure 3: Anammox two-step reaction and the respective genes catalysing each reaction.

2.3 Denitrifying bioreactors

An increased usage of nitrogen in for example agriculture and industry have resulted in an accumulation of nitrogen in the environment (Galloway *et al.* 2003). The negative impact on both terrestrial and aquatic environments have forced new technical solutions in order to address this problem. One solution is denitrifying bioreactors which have been proven capable of substantial NO_3^- removal (Schipper *et al.* 2010a). One type of denitrifying reactors are denitrification beds which are filled with a carbon source. Water with high concentration of NO_3^- flows through the bioreactor and NO_3^- is reduced to N_2 through denitrification. Denitrification beds are suggested to be a rather inexpensive technology with a passive or semi-passive system (Schipper *et al.*

2010b). With an increased usage of denitrifying bioreactors, more knowledge about which factors affecting the NO_3^- removal have become clear. The choice of carbon source determines the longevity of the bioreactor and also the availability of carbon (Grießmeier *et al.* 2019). Woodchips have shown to be a slowly degradable carbon source suited for denitrifying bacteria (Moorman *et al.* 2010, Warneke *et al.* 2011). The microbial community also plays a large role in NO_3^- removal as different organisms can perform different reactions. As previously mentioned, not all denitrifying organisms perform complete denitrification but only one step of the reaction. Therefore, differences in abundances of nitrogen-reducing organisms will affect the N removal efficiency. An important design parameter when setting up a denitrification bed is the hydraulic retention time (HRT), the time it takes for a compound to pass through the bioreactor. The HRT inside the bioreactor affects the N removal efficiency and the N removal rate (Lepine *et al.* 2016). A longer HRT results in a higher removal efficiency while a shorter HRT gives a higher removal rate. These have been shown to not always agree, the retention time for optimal N removal is not the same as the retention time for optimal N removal rate (Lepine *et al.* 2016). All these factors highly affect the performance of the bioreactor.

Unfavourable side products can be created during NO_3^- removal in denitrifying bioreactors affecting the performance. These reactions need to be considered when designing the system. For example, the greenhouse gas N_2O could be created due to organisms not capable of complete denitrification (Canfield *et al.* 2010). Another unfavourable side product could be nitrite. Accumulation of NO_2^- in a denitrification bed depends on several factors, summarised by Grießmeier *et al.* 2019. For example, NO_2^- accumulation could be due to incomplete denitrification or due to a delay in further reduction of NO_2^-, even in organisms performing complete denitrification. The toxic gas H_2S can be produced as a side product when sulphate is present in the water. Nitrate is a favoured electron acceptor in a denitrification bed, but when nitrate concentration is greatly reduced, it becomes possible for other reductions to occur, such as sulphate reduction (Grießmeier *et al.* 2019). In a pilot scale woodchip bioreactor, sulphate reduction increased under N-limiting condition (Lepine *et al.* 2016). Therefore, knowledge of the microbial community in the bioreactor increases the understanding of which potential reactions that can occur.

2.4 Quantitative real-time PCR

To quantify the abundances of functional genes in the bioreactor, quantitative real-time polymerase chain reaction (qPCR) was used. qPCR have previously been used to quantify functional genes of denitrifying bacteria in a woodchip reactor (Herbert *et al.*

2014). qPCR is used to amplify specific sequences and measure the initial amount of amplified sequence. In contrast to conventional PCR, the accumulation of PCR products can be detected as the reaction progresses. The detection of PCR product is possible due to the inclusion of a fluorescent molecule which will fluoresce when bound to the DNA (Bio-Rad Laboratories, 2006). The fluorescence signal is measured for each cycle and, more signal equals more DNA. By creating a standard curve using a template of known concentration, the fluorescence signal can be compared to the standard curve in order to determine the starting quantity of the product (Bio-Rad Laboratories, 2006).

When using double stranded DNA, creating a melt curve and performing gel electrophoresis are recommended quality controls. Gel electrophoresis will visualise the qPCR products on an agarose gel and with the use of a DNA ladder the size of the amplified products can be determined. One band of the correct size will indicate amplification of the desired fragment. However, multiple bands confirms nonspecific binding such as primer-dimer or an unwanted product. The melt curve is performed after amplification is complete. The temperature is gradually increased resulting in single stranded DNA, as double stranded DNA denature. The dye then dissociates leading to a decrease in fluorescence. A melt curve displaying the fluorescence as a function of temperature will show the melt temperature of each qPCR product (Bio-Rad Laboratories, 2006). One peak at the same temperature as the standard indicates the presence of one fragment with the correct size. Multiple peaks or differences in melt temperature between standard and the qPCR product indicates the presence of nonspecific product. The quality controls can be compared for each qPCR product.

2.5 Sulphate reduction

Sulphur is an abundant element on earth. It is commonly found as sulphate (SO_4^{2-}) in seawater, and as gypsum ($CaSO_4$) and pyrite (FeS_2) in rocks (Muyzer and Stams, 2008). Sulphate-reducing bacteria (SRB) are anaerobic microorganisms which can be found in a large variety of anoxic environments where they play a crucial role in the sulphur and carbon cycles. Sulphate is used as an electron acceptor but a variety of other molecules like organic compounds or hydrogen can also be used (Muyzer and Stams, 2008). Sulphate reduction occurs when sulphate is transformed to adenosine-5'-phosphosulphate (APS) by the ATP-sulphurylase. APS is further reduced to sulphite (SO_3^{2-}) by APS reductase. The last step of the reaction is the reduction of SO_3^{2-} to sulphide (S^2-) by dissimilatory sulphite reductase genes *dsr* (Rabus *et al.* 2004).

In the mining company LKAB, gypsum is present in the bedrock and due to precipitation gypsum is dissolved in water and later found in water discharged to the recipient (LKAB, 2020). By odour, the toxic gas H_2S was detected in the bioreactor during the summer of 2019 suggesting sulphate reduction. H_2S can cause damage in industry due to its corrosive effect (Muyzer and Stams, 2008). This raised the question of to what extent and where in the bioreactor SRB are active. Quantification of SRB have been performed in previous studies. Dissimilatory sulphite reductase is encoded by the conserved genes *dsr*, found in all sulphate-reducing organisms (Wagner *et al.*, 1998). *dsr* genes have been proven successful as genetic markers when wanting to determine the size of the SRB community (Kondo *et al.* 2004, Wagner *et al.* 1998).

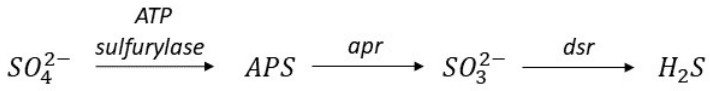

Figure 4: Dissimilatory sulphate reduction with the respective genes catalysing each reaction.

3 Materials and methods

3.1 Bacterial strains and growth conditions

Genomic DNA from *Desulfitobacterium hafniense* strain DCB-2 (DSMZ-10664) was used for amplification of dissimilatory sulphate reductase gene *dsr*. Standards with cloned DNA of 16S rRNA, *nirS, nirK, nosZ*I, *nosZ*II, *nrfA*, and *hdh* had already been prepared. *Escherichia coli* One Shot TOP10 competent cells were used for cloning. Cultivations were grown in LB medium (Difco) at 37 °C overnight.

3.2 System description

The bioreactor in the present study is situated in the mining company LKAB industrial area in Kiruna, Sweden. The bioreactor has a trapezoidal form and is situated subsurface at a depth of 2.1 meters. The dimensions at ground surface are 44 m long and 7 meters wide while the dimensions at bottom surface are 34 m long and 2 m wide (Fig. 5). Two inner walls made of plywood are located at 5 and 34 meters from the

inlet to avoid surface flow. The bioreactor is filled with pine woodchips. Groundwater, mainly leachate from the waste rock dump, is collected in a water reservoir located at the end of the waste rock pile. The water is pumped through gate valves to the bioreactor and subsequently discharged through a monitoring chamber and then further to a drainage ditch. To allow for water sampling, the bioreactor contains groundwater tubes located at five positions along the reactor length. There are two tubes per position, and they contain slits to collect water at the bottom depth and from 1 meter above bottom.

Figure 5: The bioreactor under construction in September 2018. The white tubes are the groundwater tubes. Photo: Roger Herbert.

3.3 Sampling and DNA extraction

Water was collected in 2019 between June and September at five occasions, resulting in a total of 65 water samples. At each occasion water samples were collected via the groundwater tubes at the two depths using a peristaltic pump. In addition, water samples were collected from the pump well or a close by inlet tube, and from the outlet well. A volume of approximately 2 L of water was discarded before collecting 2 L of each sample. The water was filtered through 0.2 μm pore size Sterivex® filters. DNA was extracted from the filters using the powerSoil kit (Qiagen). Both sampling and DNA extraction had already been done at the start of this thesis project.

3.4 Quantitative PCR of functional genes

Quantitative real-time PCR (qPCR) was used to determine the abundances of denitrifying, anammox, and DNRA bacteria in the bioreactor using functional genes as genetic markers. Nitrite reductase genes *nirS* (Throbäck *et al.*, 2004) and *nirK* (Henry *et al.*, 2004), and nitrous oxide reducatase gene *nosZ*I (Henry *et al.*, 2006) and *nosZ*II (Jones *et al.*, 2013) represent the potential denitrifying community, hence the genetic potential for denitrification. *nrfA* (Welsh *et al.*, 2014, Mohan *et al.*, 2004) represent the potential DNRA community and *hdh* (Schmid *et al.*, 2008) the anammox. 16S rRNA was used as proxy for the total bacterial community (Muyzer *et al.*, 1993). qPCR was performed on CFX Connect Real-Time System (Bio-Rad) using SYBR green as fluorescent detector. Two independent 15 μL reactions per sample were performed for each gene. Each reaction contained iQ SYBR Green Supermix (Bio-Rad), 0.5-2 μM of each primer, 15 μg of Bovine Serum Albumin, and 3 ng of DNA. Cycling conditions, primer sequences, and concentrations for each gene are found in appendix (Table 1). Standard curves were obtained through serial dilution of linearised plasmid containing the functional gene with a known concentration. The serial dilutions were done in the range 10^1-10^8 and demonstrated a linear relationship ($R^2 > 0.98$). The efficiency was 78, 72, 79, 92, 82, and 86 % for *nosZI, nosZII, nirS, nirK, nrfA*, and *hdh* respectively. A melt curve and gel electrophoresis were used as quality controls to verify the presence of only one amplicon of the correct size in the qPCR product. Gel electrophoresis was done to visualise the qPCR product on 1.2 % agarose gel loaded with a DNA ladder (Gene ruler 100 kb).

3.5 Data analysis

The functional genes *nirS, nirK*, *nosZ*I, *nosZ*II, *nrfA*, and *hdh* were used as genetic markers to indicate the genetic potential of each community. In order to determine the size of the community distribution, the factors length and depth of the bioreactor were used to map the abundances in a time dependent manner. Time was designated as the date the sample was collected, length in meters from the inlet, and depth as A and B (A being collected 1 meter above bottom and B at the bottom). The gene abundances were statistically tested using length, depth, and time as well as concentration levels of nitrogen and nitrous oxide (aq). All statistical analyses was performed in R.

Abundance data were not normally distributed and were therefore not applicable for parametric statistics as normality is a criterion. Hence, non-parametric (rank-based) tests were applied (alpha = 0.05). The differences between the gene abundances

collected at the two depths (A and B) were tested using a Wilcoxon rank-sum test. A Wilcoxon rank-sum test could not be used on the factors length and time as they had more than two levels. Instead a Kruskal-Wallis test was used to test significant differences between the gene abundances at different lengths and times individually. Dunn's test for multiple comparisons using a false discovery rate correction was further used to test the significant differences in gene abundances between each pairwise points of length and time, respectively (function *dunnTest*, p.max = 0.025, within R-package FSA).

Nitrogen (NO_3^-, NO_2^-, NH_4^+) concentrations were available from the same sampling time as the water samples. The data contained values below detection limit which were set to half of the detection limit as an arbitrary concentration. Spearman's rank correlation was used to evaluate the correlation between the gene abundances and the nitrogen concentrations as well as between gene abundances of different functional genes. Nitrogen concentrations below detection limit were excluded from the correlation with gene abundances resulting in 33, 31, and 51 data points for NO_3^-, NO_2^-, and NH_4^+ respectively.

Analysis of similarity with permutations (anosim, n=999) was used to statistically test the differences in abundances between and within length, time, and depth respectively, using a Bray-Curtis (BC) dissimilarity matrix. An analysis of variance tested pairwise comparisons between gene abundances collected at different lengths, depths, and times using the BC dissimilarity matrix and permutation (n=999). To illustrate the whole nitrogen community composition an ordination was produced using non-metric multidimensional scaling (NMDS) and the BC dissimilarity matrix. The NMDS included 54 water samples, excluding time points when nitrogen concentrations were not determined. Gene abundances were normalised against the quotient of 16S rRNA abundance. Nitrogen concentrations, total N removal, and N_2O (aq) removal were added to the matrix as vectors using correlation test with permutation (n=999) (function *envfit*, p.max = 0.05, within R-package vegan). The nitrogen concentrations included data of below detection limit.

3.6 Assay for quantification of sulphate-reducing bacteria

3.6.1 PCR

To set up an assay quantifying the genetic potential of the process dissimilatory sulphate reduction using qPCR, a standard plasmid is needed. Therefore, primers amplifying the genes *dsrA* or *dsrB* are necessary. Primers were selected based on

literature describing qPCR of these genes of samples from similar conditions found in the mine water. Five primer pairs where selected; DSR 1F/DSR 4R (Wagner *et al.*, 1998), DSR 1F+/DSR 4R (Kondo *et al.*, 2004), DSRp2060F/DSR 4R (Geets *et al.*, 2006), and DSR F1/RH3-dsr-R (Ben-Dov *et al.*, 2007). *Desulfitobacterium hafniense* is a sulphate-reducing bacteria and DNA from the strain DCB-2 was used as template. For PCR amplification a total reaction volume of 25 μL were performed using 10X DreamTaq Green Buffer (Thermo Scientific), 2 mM deoxynucleoside triphosphates, 0.5 μM of each primer, 1.5 U of DreamTaq DNA polymerase (Thermo Scientific), and 1-2 ng of DNA. Amplification was carried out in a T100 Thermal Cycler (Bio-Rad) with gradient annealing temperature. Initial denaturation for 3 minutes at 95 °C, amplification for 30 cycles with each cycle consisting of 95 °C for 30 s, 51-61 °C for 30 s, 72 °C for 1 minute. The extension time for 1.9 kb fragments was 2 minutes. The amplification completed with final extension at 72 °C for 20 minutes to ensure complete 3'-dA tailing of the PCR product. The PCR products were inspected on a 1.2 % agarose gel to verify correct amplicon. Primer pair DSRp2060F/DSR4R showed a band at 350 bp with a strong signal for annealing temperature of 51 °C. Neither of the other primer pairs showed the desired amplicon and were excluded from further analyses. The PCR product from DSRp2060F/DSR4R was purified using E.Z.N.A Cycle pure kit (Omega Bio-Tek). The concentration of the PCR product was measured using Qubit fluorometer (Invitrogen). A control PCR reaction was performed as suggested in the TOPO TA Cloning Kit for sequencing protocol (Thermo Scientific). The control reaction was used to evaluate the cloning result.

Table 1: Oligonucleotide sequences used for polymerase chain reaction

Primer pair	**Sequence**	**Gene**	**Fragment size (bp)**
DSR1F	ACSCACTGGAAGCACG	*dsrAB*	1900
DSR4R	GTGTAGCAGTTACCGCA		
DSR1F+	ACSCACTGGAAGCACGGCGG	*dsrAB*	1900
DSR4R	GTGTAGCAGTTACCGCA		
DSRp2060F	CAACATCGTYCAYACCCAGGG	*dsrB*	350
DSR4R	GTGTAGCAGTTACCGCA		
DSR1F	ACSCACTGGAAGCACG	*dsrA*	222
RH3-dsr-R	GGTGGAGCCGTGCATGTT		

3.6.2 Ligation, transformation and digestion

The purified PCR product and the control fragment were ligated in pCR® TOPO-4.1 plasmid vector and transformed into *Escherichia coli* One Shot TOP10 competent cells using TOPO TA cloning kit according to the manufacturer's instructions (Thermo Scientific). Two vector:insert ratios were used, 1:1 and 1:3. The ligation mixtures were incubated for 10 minutes. Three different transformation volumes (10, 50, 100 μL) were spread on respective agar plate containing kanamycin (50 μg mL^{-1}). The plates were incubated overnight at 37 °C. Colony PCR was performed to verify correct ligation using M13 primers according to the cloning kit protocol and inspected on 1.2 % agarose gel. The expected fragment was 520 bp. Colony PCR products from two colonies were purified using E.Z.N.A Cycle pure kit (Omega Bio-Tek) and sent for sequencing at Macrogen Europe using M13 primers. A sequence similarity search was performed using BLAST, with no additional settings, of the nucleotide sequence to the protein sequence database. The same clones that were sent for sequencing were incubated in LB and ampicillin (100 μg mL^{-1}) in shaker at 37 °C overnight. The plasmid was purified from the cells using QIAprep spin miniprep kit (Qiagen) and digested with the restriction enzyme NotI for 45 minutes at 37 °C and 20 minutes at 65 °C. The products were separated using gel electrophoresis and inspected on 1 % agarose gel together with respective circular plasmid. The linearised plasmid was purified using E.Z.N.A Cycle pure kit (Omega Bio-Tek).

3.6.3 Quantitative PCR of dissimilatory sulphite reductase

To test and optimise the assay, PCR was performed of the linearised and circular plasmid with two different annealing temperatures, 51 °C and 60 °C together with two different primer concentration 0.5 μM and 0.2 μM. The qPCR and PCR products were separated using gel electrophoresis and inspected on a 1 % agarose gel.

The linearised plasmid with *dsrB* was tested as a standard by performing qPCR with gradient temperature as described in section "Quantitative PCR of functional genes". Standard curves were made through serial dilutions of the linearised plasmid in the range 10^1-10^7 copies per reaction. Five water samples were included in the qPCR and used as DNA template to investigate if the primer pair DSRp2060F/ DSR 4R could amplify *dsrB* found in the bioreactor.

4 Results

4.1 Abundance and distribution of nitrogen-reducing bacteria

The abundances of nitrogen-reducing bacteria were measured in the water samples with qPCR, using functional genes as genetic markers. All functional genes, except *hdh*, confirmed only one amplicon of the desired size when performing gel electrophoresis of the qPCR products. *hdh* showed multiple fragments and was not quantifiable in any of the water samples and was therefore excluded from further analysis. The melt curve from qPCR of *nrfA* showed a different melting temperature of the amplicons in some of the water samples in comparison to the standard. As gel electrophoresis of the qPCR products visulised correct size of the amplicon, this was concluded to indicate a variation of the gene between different bacteria.

4.1.1 Temporal changes and variations at different depths

One of the aims of this project was to determine the distribution of different microbial communities in the bioreactor. Therefore, the different factors depth measured at different times are of interest in order to investigate their respective effect on the abundances. No significant differences were found between gene abundances collected at different depths, except for *nosZ*I (Appendix, Table 2), when performing a Wilcoxon rank-sum test ($p<0.05$). Hence, depth was excluded in the subsequent analyses. A Kruskal-Wallis test was used to test the differences in gene abundances collected at different times. Time was not a significant factor for gene abundances and the factor was therefore excluded in further analyses (Appendix, Table 3).

4.1.2 Spatial changes along the bioreactor length

In order to determine the distribution along the bioreactor length the factor length was also investigated. Based on a Kruskal-Wallis test, length appeared to be a factor on which all gene abundances, except *nosZ*II showed a dependence, where *nrfA* showed the highest (Appendix, Table 4, Fig. 2). In order to investigate the nature of the dependence, a Dunn's test was used to compare the abundances between each pair of lengthwise points. 16S rRNA and the functional genes *nirS*, *nosZ*I, and *nrfA* showed a significant difference in abundances between different lengths of the bioreactor. 16S rRNA, *nirS*, and *nosZ*I showed a difference between gene abundances at length 3.1 m of the bioreactor, and length 20.5 and 29.2 m. Additionally, 16S rRNA and *nosZ*I showed a difference between length 3.1 and length 37.5 m. *nrfA* showed a significant

difference between length 3.1 m as well as 11.4 m, and length 29.2 and 37.5 m (Appendix, Table 5, Fig. 2).

Figure 2 shows the abundances of 16S rRNA and the functional genes along the bioreactor length. The most abundant gene of the quantified functional genes in the bioreactor was *nosZ*II and the least abundant gene was *nirS*. Out of the nitrite reductase encoding genes, *nirK* was more abundant than *nirS* throughout the reactor while for the nitrous oxide reductase encoding genes, *nosZ* clade II was consistently more abundant than *nosZ* clade I. The 16S rRNA gene abundance initially increased and peaked at length 20.5 m of the bioreactor where it slowly started to decrease.

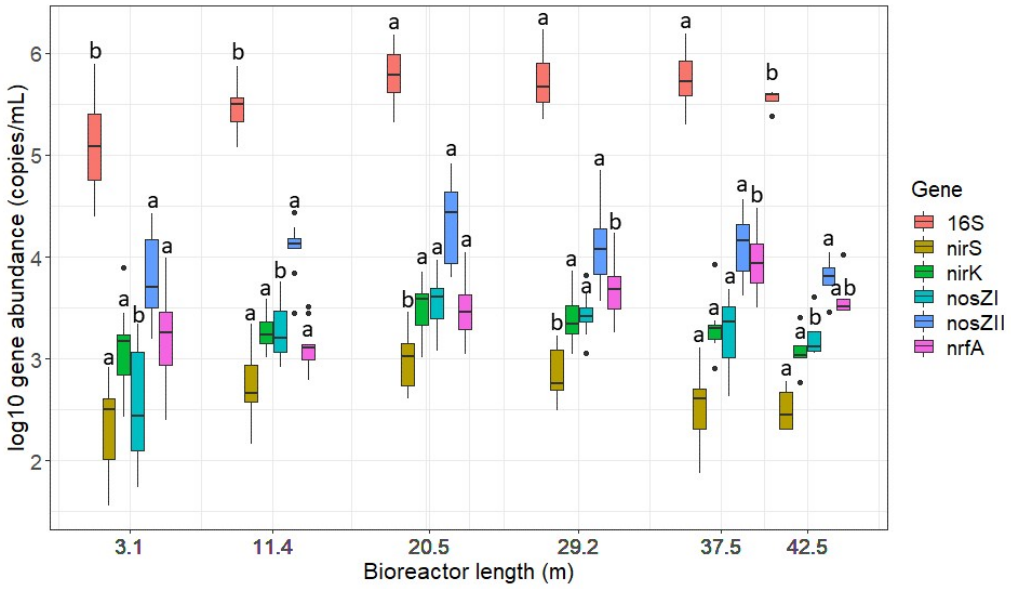

Figure 6: Abundances of functional genes along the bioreactor length. Gene abundances are log10 transformed. Different letter above the boxes indicate significant difference, per gene, in abundance across the length of the reactor and is based on the output from Dunn's test ($p<0.05$). The lower and upper hinges correspond to the the 25th and 75th percentiles. Lines through boxes are medians. Whiskers represent the min and max values excluding outliers. Outliers are represented by circles.

Genes encoding nitrite reductase (*nirS* and *nirK*) together with genes encoding nitrous oxide reductase (*nosZ*I and *nosZ*II) represent the genetic potential for denitrification. The abundance of Σ*nir*, Σ*nosZ*, and *nrfA* as a part of the total community varies along the length of bioreactor (Fig. 7). Σ*nir* and Σ*nosZ* decreases along the bioreactor length. However, the abundances of Σ*nosZ* are roughly three times larger than Σnir (Fig. 7). Nitrite reductase gene *nrfA* is used as proxy for the genetic potential of DNRA and increases halfway through the bioreactor length. Between the lengths 3.1

m to 20.5 m of the bioreactor the gene abundance is generally higher for denitrification than DNRA (Fig. 7).

Based on a Spearman correlation test, significant correlations ($p<0.05$) were detected between N concentrations and gene abundances of different functional genes. NO_3^- and NO_2^- showed a negative correlation with *nrfA* (Table 2). NO_3^- did not show a significant correlation with either *nirS* nor *nirK*, but a relatively strong correlation to the sum of Σnir (*nirS* + *nirK*) (Table 3). NH_4^+ had a positive correlation with 16S rRNA, *nirS, nirK*, and *nosZ*II (Table 2). There were also significant correlations ($p<0.05$) between different functional genes. Σnir showed a positive correlation with *nrfA*, and a strong positive correlation with Σnor (*nosZ*I + *nosZ*II) (Table 3).

The NO_3^- concentrations were most abundant at length 0 m (inlet) of the bioreactor and decreased along the length of the bioreactor. NO_2^- was found in much lower concentrations compared to NO_3^- and accumulate at length 11.4 m of the bioreactor and thereafter reduced. NH_4^+ was detected in low concentrations but appears to increase at length 20.5 m of the bioreactor. (Fig. 8). The reduction of N_2O in water can be found in appendix (Fig. 1).

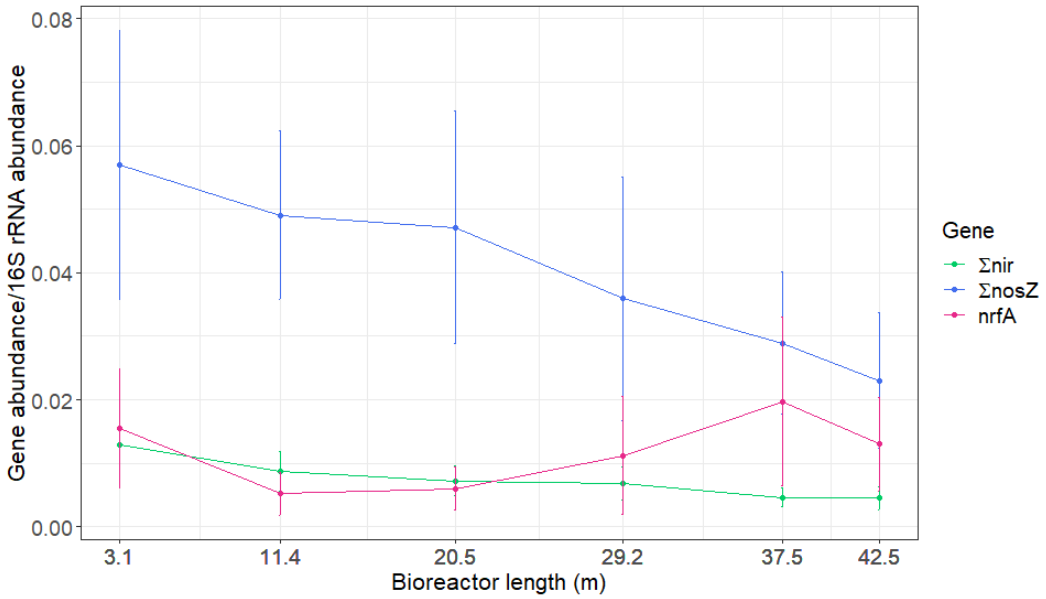

Figure 7: Dentrification and DNRA, represented by gene abundance, along the bioreactor length. The Σ nir (nirS+nirK) and ΣnosZ (nosZI+nosZII) represent the genetic potential of denitrification. The functional gene nrfA represent the genetic potential of DNRA. The gene abundance of Σnir, ΣnosZ, and nrfA are normalised against 16S rRNA abundance. The error bars represent ± standard deviation, n=55.

Table 2: Spearman's correlation analysis between abundances of 16S rRNA and functional genes (nirS, nirK, nosZI, nosZII, nrfA) and nitrogen concentration (NO3-N, NO2-N, NH4-N). The table show the probability value, p-value (top) and the correlation coefficient, rho (bottom) for each correlation. Bold represents significant correlation (p-value<0.05); n=54.

	p-value *rho*					
	16S rRNA	*nirS*	*nirK*	*nosZ*I	*nosZ*II	*nrfA*
NO3-N	**0.0344**	0.5538	0.9774	0.2532	0.5536	**0.001327**
	-0.3536	*-0.1017*	*-0.00489*	*-0.1955*	*-0.1021*	*-0.5205*
NO2-N	0.9074	0.09295	0.4554	0.4072	0.36	**0.01561**
	-0.0211	*0.2975*	*0.1345*	*0.1487*	*0.1641*	*-0.4201*
NH4-N	**0.001702**	**0.002485**	**0.0007251**	0.05339	**0.007472**	0.06411
	0.4286	*0.4146*	*0.4580*	*0.2721*	*0.3703*	*0.2612*

Table 3: Spearman's correlation analysis between abundances of the functional genes Σnir (nirS + nirK) and ΣnosZ as well as nrfA, and between the nitrate concentration, NO3-N. The table shows the probability value, p-value, (top) and the correlation coefficient, rho, (bottom) for each correlation. Bold represents significant correlation (p-value<0.05); n=54.

	p-value *rho*		
	Σ*nosZ*	*nrfA*	NO3-N
Σ*nir*	**2.2e-16**	**0.02744**	**3.939e-06**
	0.8116	*0.3059*	*0.7176*

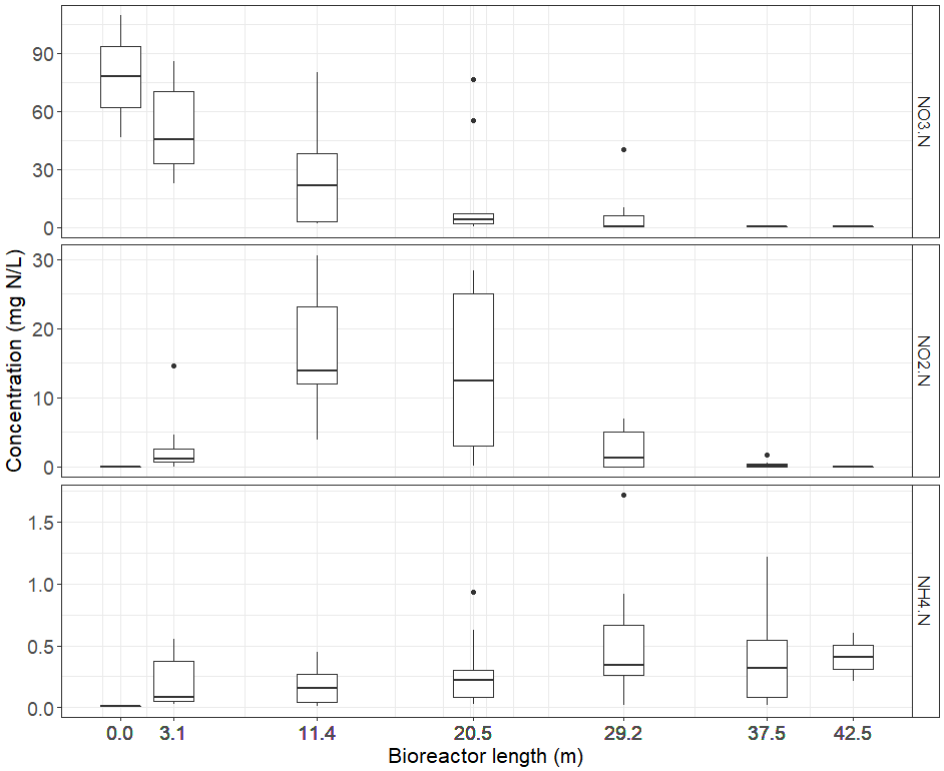

Figure 8: Concentration of nitrate (top), nitrite (middle), and ammonium (bottom) along the bioreactor length. Observe the different scales on the y-axis. The lower and upper hinges correspond to the the 25th and 75th percentiles. Lines through boxes are medians. Whiskers represent the min and max values excluding outliers. Outliers are represented by circles. The total amount of data points for nitrate, nitrite, and ammonium are 47, 38, and 53, respectively.

4.1.3 Non-metric multidimensional scaling

The ordination method NMDS illustrates the relationship between the whole nitrogen community and the factors length and depth collected at different times. The NMDS is created based on a Bray-Curtis dissimilarity matrix. No association to either depth or time could be seen (Fig. 9). The NMDS indicated a difference between length 3.1 m and the rest of the lengths. The NO_3^- level and N_2O (aq) removal appears to associate with the length 3.1 m (Fig. 9). The gene abundance at length 11.4 and 20.5 m show a tendency of clustering together. Analysis of similarity (anosim) can be coupled to a NMDS to test the significant difference in gene abundances between and within length, depth and time individually. No significant differences were detected between gene abundances of different times and depths (Appendix, Table 6). Length showed a significant difference (p-value < 0.05) suggesting an even distribution between and within the different lengths. To further investigate length as a factor of interest, a

multivariate analysis of variance was used to compare the whole community abundances between each pair of lengthwise points. The test detected a significant difference between the length 0 m (inlet) of the bioreactor and length 3.1 and 11.4 m. A difference could also be found between length 3.1 m and all other length points in the bioreactor (Table 4).

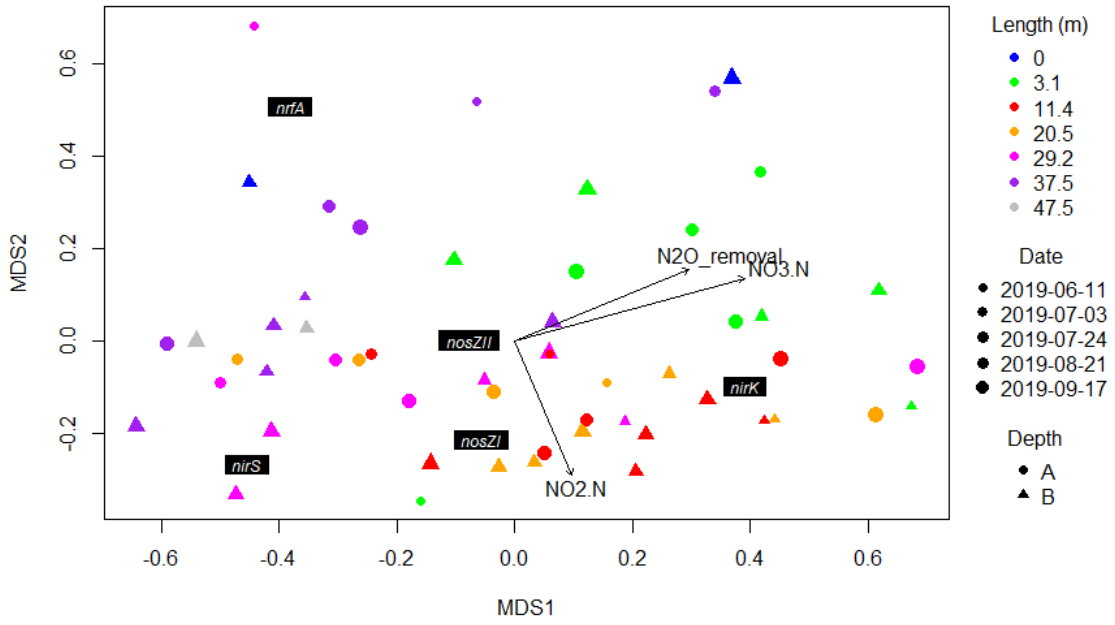

Figure 9: Non-metric multidimensional scaling based on Bray-Curtis dissimilarity matrix for the gene abundances (n=54) of the functional genes nirS, nirK, nosZI, nosZII, and nrfA. Gene abundances are normalised against the quotient of 16S rRNA gene abundances. Arrows represent significant correlation (p<0.05) of nitrate (NO3.N), nitrite (NO2.N), and N_2O (aq) reduction (N2O_removal).

Table 4: Pairwise comparisons of the community structure at each length of the bioreactor using permutational manova on a Bray-Curtis dissimilarity matrix. The Bray-Curtis dissimilarity matrix is based on gene abundances which are normalised against the quotient of 16S rRNA gene abundance. Bold represents significant p-value (<0.05).

	p-value					
	0	3.1	11.4	20.5	29.2	37.5
3.1	**0.0235**					
11.4	**0.0242**	**0.035**				
20.5	0.057	**0.035**	0.804			
29.2	0.197	**0.035**	**0.04**	0.197		
37.5	0.181	**0.014**	**0.014**	**0.014**	0.377	
42.5	0.389	**0.040**	**0.040**	0.086	0.516	0.516

4.2 Assay for quantification of sulphate-reducing bacteria

As the goal was to set up a qPCR assay determining the abundance of sulphate-reducing bacteria, a standard plasmid with a cloned fragment encoding dissimilatory sulphate reductase (*dsrA* or *dsrB*) was needed. PCR of *dsrA* and *dsrB* was performed using genomic DNA from *D. hafniense* and four potential primer pairs DSR 1F/DSR 4R, DSR 1F+/DSR 4R, DSRp2060F/DSR 4R, and DSR 1F/RH3-dsr-R. The PCR was performed with temperature gradient and the results were inspected on an agarose gel. A band was visible at 350 bp using DSRp2060F/DSR 4R, decreasing in intensity with increasing annealing temperature. The band indicates correct amplicon size of *dsrB* (Table 1). DSR 1F/DSR 4R showed two bands at 2.5 kb and at 500 bp decreasing in intensity with increasing annealing temperature, neither representing *dsrAB*. No amplification product was obtained using DSR 1F/RH3-dsr-R nor DSR 1F+/DSR 4R. The amplification of dissimilatory sulfite reductase gene *dsrB* using the primer pair DSRp2060F/DSR4R was purified and the other primers were excluded from further analysis.

Following ligation with TOPO TA cloning kit for sequencing (Thermo Scientific) the plasmid was transformed into *E. coli* One Shot TOP10 competent cells. The transformation resulted in several colonies on all plates. Agarose gel following colony PCR on twelve colonies indicated successful ligation showing a single band at 500 bp for all reactions. Two samples from the colony PCR were sent for sequencing to confirm correct ligation. The same products were linearised with NotI and confirmed the identity of the cloned fragment when inspected on agarose gel.

To optimise the assay a PCR of the circular and linearised plasmid was performed. Two different annealing temperatures were tested, 51 °and 60 °C, together with two different concentrations of the primers, 0.2 μM and 0.5 μM. The obtained agarose gel of the PCR products showed one band at 350 bp representing amplification of *dsrB*, and one at 300 bp indicating nonspecific binding.

To test whether the plasmid works as a standard for detection of *dsrB* a qPCR was performed with a temperature gradient. The standard curve did not show a linear relationship and the melt temperature of the standard plasmid and the water samples did not agree. The obtained agarose gel showed the same results as seen for the PCR with two bands.

The sequencing result confirmed correct cloning of the fragment into the plasmid. The sequence obtained with the primers DSRp2060F and DSR 4R showed good alignment with the fragment. No apparent second binding site could be found explaining the nonspecific binding. When performing a BLAST of the sequence good alignment was shown with carbamoyl-phosphate synthase large subunit from *Desulfitobacterium hafniense*.

5 Discussion

5.1 Abundance and distribution of nitrogen-reducing bacteria

The goal was to quantify the abundance and determine the distribution of different nitrogen-reducing communities in the bioreactor by using functional genes as genetic markers. 16S rRNA was used as proxy for the total bacterial community. The nitrate reductase genes *nirS* and *nirK*, and the nitrous oxide reductase genes *nosZ*I and *nosZ*II represented the genetic potential for denitrification. The nitrite reductase gene *nrfA* represented the genetic potential for DNRA. The functional gene *hdh* was used as proxy for anammox however, no genetic potential for anammox was detected.

Different statistical tests indicated that the distribution of the different communities were not affected by depth or time. The NMDS also validated how time and depth are not factors affecting the distribution when observing the whole community. However, the size of the total bacterial community increased with length of the bioreactor and were significantly different between the start and the middle. The functional genes *nirK, nosZ*I, and *nrfA* had significant differences in gene abundances along the

bioreactor length. The differences were generally seen between the start of the bioreactor and the middle. This was also validated by the NMDS where gene abundances at length 3.1 m of the bioreactor appeared to cluster alone, differing in abundances in comparison to the other lengths. Abundances at length 11.4 m appeared to cluster together with 20.5 m indicating similar composition and this was confirmed by the permutational test. Therefore, length affected the distribution of gene abundances at least for some functional genes, suggesting that environmental conditions differed along the bioreactor length.

The main nitrogen-reducing process in the bioreactor appeared to be denitrification since NO_3^- reduced along the bioreactor length and the abundances of the functional genes involved in the denitrification pathway were higher compared to DNRA. This is in line with a previous study of nitrate-reduction of mine water (Nordström and Herbert *et al.* 2017). There was a positive correlation between the concentration of NO_3^- and NO_2^- reducers indicating that NO_2^- reduction is controlled by the concentration of NO_3^-. NO_2^- was found in much lower concentrations than NO_3^- and accumulated in the middle of the bioreactor. A possible explanation for the low concentrations could be that NO_2^- is reduced to N_2O almost immediately and is therefore not detected. The gradual increase of NO_2^- could be due to that some organisms capable of complete denitrification still accumulate NO_2^- before it is further reduced (Grießmeier *et. al* 2019). Another possible explanation could be that the availability of carbon was limited in the beginning of the bioreactor. Reduction of NO_3^- gives more energy than NO_2^- and as long as there is an excess of NO_3^-, NO_3^- reduction will be more favourable than NO_2^-, leading to NO_2^- accumulation (Grießmeier *et al.* 2019). However, the accumulation of NO_2^- is not considered as a problem since NO_2^- is reduced before leaving the bioreactor.

The NH_4^+ concentration and the functional gene *nrfA* increased halfway through the bioreactor which indicated DNRA. However, the increase of NH_4^+ was very small. The correlation between NH_4^+ and *nrfA* was weakly significant (p-value = 0.06) showing a tendency of correlating. Hence, this could be an indication that the increase in *nrfA* contributes to the process DNRA. DNRA is preferred over denitrification when there is an excess of electron donors in relation to NO_3^- (Kuypers *et al.* 2018). This is in line with what can be seen in the bioreactor but cannot be validated as total organic carbon in the water was not measured. There was a negative correlation between *nrfA* and NO_3^- as well as NO_2^- which could explain the increase in *nrfA* as NO_3^- decreased along the bioreactor length, creating a high C/NO_3^- ratio. Due to the low increase of NH_4^+ and higher NO_3^- reduction, denitrification appears to be the main nitrogen-reducing process. However, DNRA occurred at the end of the bioreactor when NO_3^- had decreased but the significance of this reaction is not determined. There could be a potential sink of ammonium in the bioreactor as organisms use ammonium for growth.

The concentration of produced ammonium may therefore be higher than what could be detected. Hence, the activity of DNRA may be of larger significance than what is predicted here.

Organisms performing denitrification do not necessarily perform the whole process but only certain reactions. The abundance of *nosZ* was higher along the bioreactor length in comparison to *nir*. The difference in abundances indicates that there are many organisms capable of N_2O reduction in the bioreactor not carrying the *nir* gene. In a study, the occurrence of *nosZ* in different organisms were investigated through comparative phylogenetic analysis. 30 % of organisms possessing *nosZ* did not have either *nirS* or *nirK* (Graf *et al.* 2014). Organisms carrying *nosZ* appears to have been favoured in the reactor and indicates that the bioreactor is efficient in reducing N_2O to N_2. This is favourable as production of N_2O is an unwanted side reaction. Unfortunately, N_2O levels were not analysed on a length scale, so no correlation between N_2O (aq) and *nosZ* was possible. This means that a conclusion cannot be drawn as to whether the abundance of *nosZ* correlates with the reducing levels of N_2O along the bioreactor length.

There were statistical differences between *nirS* and *nirK* abundances along the bioreactor length, where *nirS* was found in lower abundances than *nirK*. The NO_2^- reductase gene *nirS* is likely to have a higher frequency of co-occuring with *nosZ* in comparison to *nirK* (Graf *et al.* 2014). *nirS* almost always co-occured with nitric oxide reductase, *nor*. Thus, *nirS* denitrifiers could be more capable of performing complete denitrification (Graf *et al.* 2014). The lower abundance of *nirS* indicates that complete denitrification may not be favoured in the bioreactor, but this needs to be further analysed. A difference in gene abundances was also seen between *nosZ*I and *nosZ*II along the bioreactor length, where *nosZ*II was most abundant. An organism containing *nosZ*II is more likely to be a non-denitrifying organism producing N_2O. The high abundance of Σ*nosZ* could be an indication of denitrifying bacteria capable of reducing N_2O to N_2 (Graf *et al.* 2014). However, to draw any conclusion the bacterial genome of the water of the bioreactor needs to be analysed.

In a previous study, the abundances of the microbial communities were determined in a bioreactor installed at the LKAB industrial area, reducing nitrogen from water collected from a clarification pond. The sediment in the clarification pond contains, among others, carbon. This creates different conditions for the microorganisms, affecting the composition of the microbial communities, as well as the water composition of the influent to the bioreactor. Abundances of the functional genes were opposite of what was seen in this thesis. There was a higher abundances of *nir* in comparison to *nosZ* and the abundances of *nirS* were higher than *nirK* (unpublished data). The bioreactor in the present thesis collects water directly from the waste rock

pile. Hence, the differences between the two bioreactors could be due to large differences in microbial community and water composition between the clarification pond and water coming directly from the waste rock piles.

Even though an assay quantifying sulphate-reducing bacteria was not set up, it is interesting to discuss how sulphate reduction can occur in the bioreactor. At the same time as DNRA is indicated to have increased due to decrease in NO_3^-, sulphate reduction also becomes possible from the middle of the bioreactor. DNRA and sulphate reduction are unwanted reactions in the bioreactor. Under optimal operation complete NO_3^- removal should be accomplished at the outlet of the bioreactor. Then, NO_3^- concentrations would not decrease so quickly that DNRA and sulphate reduction would occur. This could potentially be accomplished by altering the hydraulic retention time in the bioreactor.

The nitrogen removal efficiency is dependent on the HRT in the bioreactor (Lepine *et al.* 2016). A lower water flow increases the HRT which leads to a higher N removal efficiency. However, it can also create NO_3^- limiting conditions, which may lead to other reducing reactions (Lepine *et al.* 2016). During the first operational year the water flow to the bioreactor was occasionally low due to small amounts of precipitation. The HRT was therefore higher than desired leading to low concentrations of NO_3^- as early as halfway through the bioreactor. If the collection of groundwater from the waste rock piles are not sufficient to keep an adequate flow rate to the bioreactor its performance will decrease. If a consistent flow is not possible then its performance may be improved by decreasing the length of the bioreactor. However, since there was an accumulation of NO_2^- in the middle of the bioreactor there is a risk of NO_2^- not being completely reduced the length decreased. Another option would be to have a second water source to compensate when the water flow is low. To handle variations in precipitation, different operational conditions may be needed in order to maintain a high efficiency without producing unwanted side products. Therefore, it is important to understand the microbial community, and to be able to maintain a steady HRT to achieve the best performance.

5.2 Dissimilatory sulphate reductase

The second goal of this thesis was to set up a qPCR assay to quantify dissimilatory sulphate reduction in the bioreactor. Sulphate-reducing bacteria had not been quantified in the bioreactor before but sulphate concentrations and the odour of hydrogen sulphide have been detected. Sulphate reduction is an unwanted side reaction and quantifying the sulphate-reducing community would contribute to a better

understanding of the bioreactors' performance. The purpose of the NITREM project is to reduce nitrogen concentration but not at the cost of creating a new problem.

A plasmid containing the dissimilatory sulphate reductase gene *dsrB* was constructed using *D. hafniense* strain DCB-2 as template. When testing the plasmid as a standard by using PCR and qPCR amplification resulted in two amplicons, one likely representing *dsrB* and the other a product from nonspecific binding of the primers. Optimising the assay by testing a higher annealing temperature, also in combination with different primer concentrations, did not remove the nonspecific binding. qPCR was also performed on five water samples where the melt curve from the qPCR showed a different melt temperature for the standard plasmid amplicon in comparison to the water samples. The gene *dsrB* of *D. hafniense* appeared to differentiate from the genes in the bioreactor. The agarose gel also showed two amplicons.

The primer pair DSRp2060F and DSR 4R was not suited to estimate the size of the sulphate-reducing community in the bioreactor. *D. hafniense* may also not have been the best choice of template, but it was used since the DNA from the organism was readily available. However, the method of cloning a functional gene into a plasmid to create a standard was successful and resulted in a plasmid containing the desired fragment. Since it is unclear which bacteria that are responsible for sulphate reduction in the bioreactor, another approach would have been to create a standard plasmid using PCR product directly from the water samples.

5.3 Future studies

A previous bioreactor installed at LKAB reduced nitrogen from water collected from the clarification pond (Nordström and Herbert, 2018). Data from the bioreactor showed differences in the microbial community between different operational years where the changes in abundance of functional genes were associated to the concentrations of NO_3^- and temperature (unpublished data). In comparison, the present bioreactor collects water directly from the waste rock pile and nitrogen is reduced before it is released to the environment. The data presented is collected from the first operational year of the bioreactor. In order to sustain good operational conditions, more long-term changes need to be investigated. In the summer of 2020, new water samples will be collected and data from the two years will be compiled and analysed together. Additionally, woodchips from the bioreactor will be analysed and contribute to a more complete picture of the community composition. Changes in the microbial community could alter the NO_3^- removal efficiency and hence the performance of the bioreactor. Quantification of sulphate-reducing bacteria would also increase the

understanding of the bioreactor performance, explaining where and to what extent the sulphate reduction occurs. Further studies would thus contribute to an increased understanding of which temporal changes that affect the microbial community in the bioreactor. Based on this, improvements can be performed to make the bioreactor a long-term solution for reduction of nitrogen from mine water.

6 Conclusions

In this master thesis it was concluded that length of the bioreactor appeared to affect the distribution of 16S rRNA and the functional genes *nirK, nosZ*I, and *nrfA*. Denitrification was suggested as the main NO_3^--reducing process in the bioreactor. DNRA was indicated at the end of the bioreactor as the concentration of NO_3^- had decreased and a small increase of NH_4^+ was detected. The community composition in the bioreactor indicated of being efficient in N_2O as the abundance of *nosZ* was considerably larger than *nir*. To understand the temporal changes of the bioreactor further analysis are needed. The microbial community may alter with time which will affect the performance.

The assay for sulphate-reducing organisms was not possible to set up. The primer pair chosen was not suitable to detect SRB in the bioreactor as two fragments were amplified using qPCR. The choice of *Desulfitobacterium hafniense* may not have been a suitable template for cloning *dsrB*. To draw any final conclusion further analysis is needed.

7 References

Ben-Dov E, Brenner A, Kushmaro A. 2007. Quantification of Sulfate-Reducing Bacteria in Industrial Wastewater, by Real-Time Polymerase Chain Reaction (PCR) Using dsrA and apsA Genes. Microbial Ecology 54: 439–451.

Canfield DE, Glazer AN, Falkowski PG. 2010. The Evolution and Future of Earth's Nitrogen Cycle. Science 330: 192–196.

Galloway JN, Aber JD, Erisman JW, Seitzinger SP, Howarth RW, Cowling EB, Cosby BJ. 2003. The Nitrogen Cascade. BioScience 53: 341–356.

Geets J, Borremans B, Diels L, Springael D, Vangronsveld J, van der Lelie D, Vanbroekhoven K. 2006. DsrB gene-based DGGE for community and diversity surveys of sulfate-reducing bacteria. Journal of Microbiological Methods 66: 194–205.

Graf DRH, Jones CM, Hallin S. 2014. Intergenomic Comparisons Highlight Modularity of the Denitrification Pathway and Underpin the Importance of Community Structure for N2O Emissions. PloS One, 9(12), e114118. https://doi.org/10.1371/journal.pone.0114118

Grießmeier V, Leberecht K, Gescher J. 2019. NO3− removal efficiency in field denitrification beds: key controlling factors and main implications. Environmental Microbiology Reports 11: 316–329.

Hav och Vatten Myndigheten. 2020a. Miljömål och direktiv. WWW-dokument https://www.havochvatten.se/hav/samordning–fakta/miljomal–direktiv.html. Accessed: 2020-05-21.

Hav och Vatten Myndigheten. 2020b. Årlig uppföljning av miljömålen. WWW-dokument https://www.havochvatten.se/hav/samordning–fakta/miljomal–direktiv/sveriges-miljomal/arlig-uppfoljning-av-miljomalen.html. Accessed: 2020-05-21.

Henry S, Baudoin E, López-Gutiérrez JC, Martin-Laurent F, Brauman A, Philippot L. 2004. Quantification of denitrifying bacteria in soils by nirK gene targeted real-time PCR. Journal of Microbiological Methods 59: 327–335.

Henry S, Bru D, Stres B, Hallet S, Philippot L. 2006. Quantitative Detection of the nosZ Gene, Encoding Nitrous Oxide Reductase, and Comparison of the Abundances of

16S rRNA, narG, nirK, and nosZ Genes in Soils. Applied and Environmental Microbiology 72: 5181–5189.

Herbert RB, Winbjörk H, Hellman M, Hallin S. 2014. Nitrogen removal and spatial distribution of denitrifier and anammox communities in a bioreactor for mine drainage treatment. Water Research 66: 350–360.

Kondo R, Nedwell DB, Purdy KJ, Silva SQ. 2004. Detection and Enumeration of sulphate -Reducing Bacteria in Estuarine Sediments by Competitive PCR. Geomicrobiology Journal 21: 145–157.

Kuypers MMM, Marchant HK, Kartal B. 2018. The microbial nitrogen-cycling network. Nature Reviews Microbiology 16: 263–276.

Jones CM, Graf DR, Bru D, Philippot L, Hallin S. 2013. The unaccounted yet abundant nitrous oxide-reducing microbial community: a potential nitrous oxide sink. The ISME Journal 7: 417–426.

Lepine C, Christianson L, Sharrer K, Summerfelt S. 2016. Optimizing Hydraulic Retention Times in Denitrifying Woodchip Bioreactors Treating Recirculating Aquaculture System Wastewater. Journal of Environmental Quality 45: 813–821.

Lindeström, L, 2012. Kväveutsläpp från gruvindustrin. Stockholm: SveMin.

LKAB. 2019a. LKAB Miljörapport Kiruna 2019. LKAB

LKAB. 2019b. LKAB Års- och Hållbarhetsredovisning 2019. LKAB.

LKAB. Utsläpp. WWW-dokument: https://www.lkab.com/sv/hallbarhet/miljo/utslapp/. Accessed: 2020-05-24.

Mattila K, Zaitsev G, Langwaldt J. 2007. Biological removal of nutrients from mine waters. Biologinen ravinteiden poisto kaivosvedestä. Finnish Forest Research Institute.

Mohan SB, Schmid M, Jetten M, Cole J. 2004. Detection and widespread distribution of the nrfA gene encoding nitrite reduction to ammonia, a short circuit in the biological nitrogen cycle that competes with denitrification. FEMS Microbiology Ecology 49: 433–443.

Moorman TB, Parkin TB, Kaspar TC, Jaynes DB. 2010. Denitrification activity, wood loss, and N2O emissions over 9 years from a wood chip bioreactor. Ecological Engineering 36: 1567–1574.

Muyzer G, Stams AJM. 2008. The ecology and biotechnology of sulphate -reducing bacteria. Nature Reviews Microbiology 6: 441–454.

Muyzer G, Waal EC de, Uitterlinden AG. 1993. Profiling of complex microbial populations by denaturing gradient gel electrophoresis analysis of polymerase chain reaction-amplified genes coding for 16S rRNA. Applied and Environmental Microbiology 59: 695–700.

Naturvårdsverket. 2013. Sweden's environmental objectives: an introduction. Swedish Environmental Protection Agency, Stockholm.

Nilsson L, Widerlund A. 2017. Tracing nitrogen cycling in mining waters using stable nitrogen isotope analysis. Applied Geochemistry 84: 41–51.

NITREM. Om NITREM. WWW-dokument: https://nitrem.eu/om-nitrem-2/. Accessed 2020-02-06.

Nordström A, Herbert RB. 2018. Determination of major biogeochemical processes in a denitrifying woodchip bioreactor for treating mine drainage. Ecological Engineering 110: 54–66.

R core team. 2020. R: A language and environment for statistical computing. R Foundation for Statistical Computing. R Foundation for Statistical Computing, Vienna, Austria. URL: http://www.R-project.org/.

Rabus R, Ruepp A, Frickey T, Rattei T, Fartmann B, Stark M, Bauer M, Zibat A, Lombardot T, Becker I, Amann J, Gellner K, Teeling H, Leuschner WD, Glöckner F-O, Lupas AN, Amann R, Klenk H-P. 2004. The genome of Desulfotalea psychrophila, a sulfate-reducing bacterium from permanently cold Arctic sediments. Environmental Microbiology 6: 887–902.

Bio-Rad Laboratories, Inc. 2006. Real-Time PCR applications guide.

Schipper LA, Robertson WD, Gold AJ, Jaynes DB, Cameron SC. 2010a. Denitrifying bioreactors—An approach for reducing nitrate loads to receiving waters. Ecological Engineering 36: 1532–1543.

Schipper LA, Cameron SC, Warneke S. 2010b. Nitrate removal from three different effluents using large-scale denitrification beds. Ecological Engineering 36: 1552–1557.

Schmid MC, Hooper AB, Klotz MG, Woebken D, Lam P, Kuypers MMM,

Pommerening-Roeser A, Camp HJMOD, Jetten MSM. 2008. Environmental detection of octahaem cytochrome c hydroxylamine/hydrazine oxidoreductase genes of aerobic and anaerobic ammonium-oxidizing bacteria. Environmental Microbiology 10: 3140–3149.

Throbäck IN, Enwall K, Jarvis Å, Hallin S. 2004. Reassessing PCR primers targeting nirS, nirK and nosZ genes for community surveys of denitrifying bacteria with DGGE. FEMS Microbiology Ecology 49: 401–417.

Wagner M, Roger AJ, Flax JL, Brusseau GA, Stahl DA. 1998. Phylogeny of Dissimilatory Sulfite Reductases Supports an Early Origin of sulphate Respiration. Journal of Bacteriology 180: 2975.

Warneke S, Schipper LA, Matiasek MG, Scow KM, Cameron S, Bruesewitz DA, McDonald IR. 2011. Nitrate removal, communities of denitrifiers and adverse effects in different carbon substrates for use in denitrification beds. Water Research 45: 5463–5475.

Welsh A, Chee-Sanford JC, Connor LM, Löffler FE, Sanford RA. 2014. Refined NrfA Phylogeny Improves PCR-Based nrfA Gene Detection. Applied and Environmental Microbiology 80: 2110–2119.

8 Appendix

In this appendix primer sequences and concentrations can be found, as well as the output from statistical analysis using Wilcoxon rank-sum test, Kruskal-Wallis and Dunn's test are presented.

Table 1. Primers and reaction conditions for qPCR.

Gene	Primer pair	Primer sequence	Final conc	Melting		Annealing		Elongation		Data acquisition		Cycles[a]
	Forw/Rev	5´- 3´	(µM)	T (°C)	t (s)	T (°C)	t (s)	T (°C)	t (s)	T (°C)	t (s)	
16S rRNA	341F	CCTACGGGAGGCAGCAG	0.50	95	15	60	30	72	30	78	5	35
	534R	ATTACCGCGGCTGCTGGCA	0.50									
nirS	Cd3aFm	AACGYSAAGGARACSGG	0.50	95	15	65-60[b]	30	72	30	80	5	35
	R3cdm	GASTTCGGRTGSGTCTTSAYGAA	0.50									
nirK	876F	ATYGGCGGVCAYGGCGA	0.5	95	15	63-58[b]	30	72	30	80	5	35
	1040R	GCCTCGATCAGRTTRTGGTT	0.5									
*nosZ*I	1840F	CGCRACGGCAASAAGGTSMSSGT	0.50	95	15	65-60[b]	30	72	35	80	15	43
	2090R	CAKRTGCAKSGCRTGGCAGAA	0.50									
*nosZ*II	nosZIIF	CTIGGICCIYTKCAYAC	2.00	95	15	54	30	72	45	80	5	40
	nosZIIR	GCIGARCARAAITCBGTRC	2.00									
hdh	hzocl1F1	TGYAAGACYTGYCAYTGG	0.80	95	15	52.5	30	77	30	77	30	35
	hzocl1	ACTCCAGATRTGCTGACC	0.80									
nrfA	nrfAF2aw	CARTGYCAYGTBGARTA	0.50	95	15	57-52[b]	30	72	30	80	10	45
	nrfAR1	TWNGGCATRTGRCARTC	0.50									

a - Protocols start with an activation step, 95 °C for 5 minutes and are finished with a melt curve, 15 s at 95 °C followed by 65-95 °C in 0.5 °C increments for 5 s.
b - 1 °C decrease per cycle the first six cycles.

Table 2: Two-sided Wilcoxon rank-sum test between abundances of 16S rRNA and functional genes (nirS, nirK, nosZI, nosZII, nrfA) collected at different depths of the bioreactor. Bold represents significant p-value (<0.05); n=62, degrees of freedom = 1.

Gene	**p-value**
16S rRNA	0.305
nirS	0.07551
nirK	0.6536
*nosZ*I	**0.02668**
*nosZ*II	0.3646
nrfA	0.1695

Table 3: Kruskal-Wallis test between abundances of 16S rRNA and functional genes (nirS, nirK, nosZI, nosZII, nrfA) collected at different times. p-value<0.05; n=62

Gene	χ^2	**df**	**p-value**
16S rRNA	6.7872	4	0.1476
nirS	2.5167	4	0.6417
nirK	4.2775	4	0.3697
*nosZ*I	1.1048	4	0.8935
*nosZ*II	9.4458	4	0.05087
nrfA	3.6079	4	0.4617

Table 4: Kruskal-Wallis test between abundances of 16S rRNA and functional genes (nirS, nirK, nosZI, nosZII, nrfA) collected at different lengths of the bioreactor. Bold indicates significant p-value (<0.05); n=62)

Gene	χ^2	**df**	**p-value**
16S rRNA	19.538	5	**0.001526**
nirS	16.089	5	**0.006596**
nirK	11.547	5	**0.04155**
*nosZ*I	20.384	5	**0.001058**
*nosZ*II	9.5229	5	0.08994
nrfA	27.077	5	**5.51e-05**

Table 5: Dunn's test of multiple comparisons of abundances collected at different lengths of the bioreactor, for 16S rRNA and each functional gene (nirS, nirK, nosZI, nosZII, nrfA). Bold represents significant p-value (<0.025)

		p-value				
Gene	**↓ Length →**	3.1	11.4	20.5	29.2	37.5
	11.4	0.1655				
	20.5	**0.0023**	0.0533			
16S rRNA	29.2	**0.0039**	0.1021	0.4079		
	37.5	**0.0032**	0.0840	0.4495	0.4635	
	42.5	0.2886	0.4915	0.1859	0.2285	0.2173
	11.4	0.1122				
	20.5	**0.0061**	0.1055			
nirS	29.2	**0.0198**	0.2291	0.3317		
	37.5	0.2714	0.2702	0.0256	0.0840	
	42.5	0.4391	0.2786	0.1125	0.1361	0.4101
	11.4	0.2450				
	20.5	0.0418	0.1157			
nirK	29.2	0.1105	0.2057	0.2765		
	37.5	0.1909	0.3644	0.1704	0.2842	
	42.5	0.1997	0.1160	0.0747	0.0691	0.1063
	11.4	0.0297				
	20.5	**0.0001**	0.0758			
*nosZ*I	29.2	**0.0098**	0.3438	0.1637		
	37.5	**0.0230**	0.4239	0.0973	0.3669	
	42.5	0.3169	0.3498	0.1073	0.2922	0.3622
	11.4	0.1727				
	20.5	0.0455	0.2937			
*nosZ*II	29.2	0.2415	0.4706	0.1922		
	37.5	0.2776	0.4561	0.1703	0.4542	
	42.5	0.3996	0.1626	0.1503	0.1678	0.2062
	11.4	0.2710				
	20.5	0.1639	0.0550			
nrfA	29.2	**0.0194**	**0.0033**	0.1582		
	37.5	**0.0005**	**0.0000**	**0.0214**	0.1704	
	42.5	0.2072	0.1767	0.4107	0.3442	0.1625

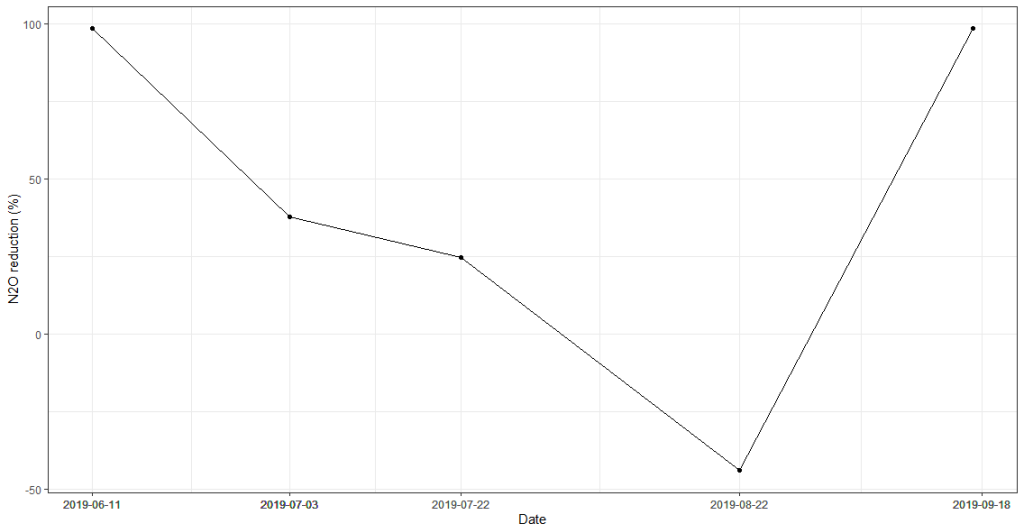

Figure 1: N_2O removal (%) in water at the sampling occasions.

Table 6: Analysis of similarity, anosim, of abundances collected at different lengths, times and depths. Bold indicates significant p-value (<0.05); n=55

Variable	**R statistics**[1]	**Significance**
Length	0.1017	**0.014**
Time	0.0185	0.196
Depth	0.005217	0.386

1. R statistics will be in the interval -1 to 1. R statistics close to 1 indicates dissimilarity between groups, R statistics close to 0 indicates random dissimilarity between and within a variable, R statistics < 0 indicates larger dissimilarity within a variable than between.